Talanta 309 (2026) 129962

Contents lists available at ScienceDirect

Talanta

journal homepage: www.elsevier.com/locate/talanta

Electrochemical viscosity correction for robust salivary ionomics via redox probe voltammetry

Hironori Myochin [a], Romanas Chaleckis [b], Tadaharu Ueda [c,d,e], Miguel Gonzálvez Noguera [f], Jie Zhang [f], Noriyasu Ohshima [g], Takashi Izumi [h], Tatsuya Hisajima [h], Mikaru Mori [a], Tomoya Kimura [a], Masanobu Mori [a,*]

[a] Department of Chemistry and Life Science, Faculty of Science and Technology, Kochi University, 2-5-1, Akebono-cho, Kochi, 780-8520, Japan
[b] Graduate School of Medical Sciences, Nagoya City University, 1 Kawasumi, Mizuho-cho, Mizuho-ku, Nagoya, 467-8601, Japan
[c] Department of Marine Resource Science, Faculty of Agriculture and Marine Sciences, Kochi University, Nankoku, 783-8502, Japan
[d] Marine Core Research Institute, Kochi University, Nankoku, 783-8502, Japan
[e] MEDi Center, Kochi University, Kochi, 780-0842, Japan
[f] School of Chemistry, Monash University, Clayton, Victoria, 3800, Australia
[g] Department of Biochemistry, Gunma University Graduate School of Medicine, Maebashi, Gunma, 371-8511, Japan
[h] Faculty of Health Care, Teikyo Heisei University, 2-51-4, Higashiikebukuro, Toshima-ku, Tokyo, 170-8445, Japan

ARTICLE INFO

Keywords:
Cyclic voltammetry
Capillary electrophoresis
Salivary ions
Salivary viscosity
Matrix effects

ABSTRACT

Accurate quantification of small ions in mucin-rich biofluids such as saliva is often compromised by viscosity-dependent diffusion effects. We propose an electrochemical viscosity-correction strategy based on the peak potential separation (ΔE_p) of the redox probe $[Fe(CN)_6]^{3-/4-}$ measured by cyclic voltammetry. The ΔE_p value under the fixed experimental conditions reflected sample-specific diffusion behavior and was employed as a correction factor for ion concentrations determined by capillary electrophoresis (CE). The relationship between ΔE_p and mucin concentration was validated using model viscosity standards, demonstrating a strong logarithmic correlation within physiologically relevant ranges. Application of the ΔE_p-based correction reduced dispersion of salivary ion measurements compared with conventional normalization approaches such as specific gravity and total protein correction. The analytical utility of the method was first examined through repeated measurements in a single individual undergoing a cold pressor test (CPT). Furthermore, its robustness was evaluated in an independent cohort of 12 healthy participants (6 cold stimulation and 6 control participants), where corrected ion profiles showed clearer differentiation between experimental conditions than uncorrected data. This ΔE_p-based correction approach provides a rapid, non-destructive, and low-volume (10 μL) analytical strategy to minimize viscosity-induced bias in ion analysis of complex biological matrices. The method enhances the robustness of CE-based ionomics and offers a broadly applicable framework for analytical measurements in non-Newtonian biofluids.

1. Introduction

Body fluids such as blood, urine, saliva, sweat, and tears are widely used as diagnostic matrices because they contain a variety of metabolites, electrolytes, proteins, and other biomolecules that reflect physiological and pathological states [1]. Their analyses support a range of applications, including disease diagnosis, therapeutic monitoring, nutritional assessment, and stress evaluation [2]. In particular, small inorganic ions and low-molecular-weight organic ions play crucial roles in maintaining osmotic balance, regulating cellular signaling, and supporting metabolic activity [3]. Therefore, accurately quantifying these ions is essential for clinical and metabolic studies.

However, ion analysis in body fluids is complicated by matrix effects. Macromolecules such as proteins and glycoproteins interfere with electrophoretic or chromatographic separations by altering ion mobility [4]. These effects are particularly pronounced in non-Newtonian biofluids such as saliva, sputum, or synovial fluid [5]. Such viscosity-related biases can obscure true biological differences and decrease the

* Corresponding author.
E-mail address: mori@kochi-u.ac.jp (M. Mori).

https://doi.org/10.1016/j.talanta.2026.129962
Received 9 March 2026; Received in revised form 1 May 2026; Accepted 8 May 2026
Available online 9 May 2026

reliability of biomarkers.

Recently, saliva has attracted increasing attention as a diagnostic biofluid for stress assessment, infectious disease screening, and monitoring of health conditions [6]. Saliva sampling is non-invasive and painless, making it better suited for point-of-care testing than blood sampling [7–9].

Numerous salivary biomarkers have been identified, such as cortisol [10–12], α-amylase [12,13], and secretory immunoglobulin A [1114–16], typically measured by enzyme-linked immunosorbent assays [17–20], colorimetric methods [21,22], or mass spectrometry [23–25]. Inorganic and small organic ions have been investigated owing to their high abundance and physiological relevance [3,26]. They have been analyzed using techniques such as capillary electrophoresis (CE) [27,28], ion chromatography [29,30], ion-selective electrodes [31,32], and colorimetric assays [33,34].

Our group developed CE-based multi-ion profiling methods for saliva [35–38], which have been used to monitor salivary ion changes in relation to food intake, smoking [35,36], weight loss in wrestlers [37], and physical exercise [38]. More recently, we introduced a CE system with a triple-layer chemically modified capillary incorporating multiple ionic polymers that effectively analyzed salivary anions and cations in 4 min each [39].

However, salivary ion concentrations vary between samples collected from the same individual under similar conditions. This variation is attributed to mucins (glycoproteins such as MUC5B and MUC7) [40,41], which affect salivary viscosity and interact with inorganic ions via functional groups such as sialic acids [40]. High mucin content can cause diffusion retardation and peak broadening, potentially affecting the apparent quantification of ions in CE analysis [42,43].

Conventional normalization methods including internal standardization [44], specific gravity (SG) adjustment [45], total protein (TP) correction [46], and total solute content normalization [47] have primarily been developed for low-viscosity fluids such as urine and sweat [48]. Their utility is limited in saliva and other viscous, non-Newtonian fluids as they do not directly address macromolecule-induced diffusion effects. A rheometric viscosity measurement can quantify such effects, but it requires a larger volume of sample [49,50].

Electrochemical methods provide an alternative for indirect assessment of matrix effects in small volumes. In cyclic voltammetry (CV), the peak potential separation (ΔE_p) is influenced by both diffusion and electron transfer kinetics [51–53]. Therefore, ΔE_p can serve as a practical correction factor reflecting matrix-induced effects on electrochemical response, rather than a direct measure of viscosity alone.

In this study, we used potassium ferricyanide as a redox probe to determine ΔE_p in a low-viscosity reference electrolyte ($\Delta E_{p,0}$) and in the same electrolyte with added saliva ($\Delta E_{p,i}$). The resulting ratio of $\Delta E_{p,r} = \Delta E_{p,0}/\Delta E_{p,i}$ was applied as a CF to adjust salivary ion concentrations measured by CE. The relationship between ΔE_p and mucin-induced matrix effects was validated using mucin and methyl cellulose standards. Then, we applied the CF to saliva samples collected before and after the cold pressor test (CPT), which is a physiological model of acute stress on sympathetic nervous function [54,55]. The performance of the CF method was compared with those of SG and TP-based normalization approaches in reducing inter-sample variability and improving the detection of stress-related ions.

2. Materials and methods

2.1. Reagents and solutions

All reagents were of analytical or biochemical grade. Electrolyte solutions were prepared from phosphate-buffered saline (PBS), potassium ferricyanide (PF), and KCl in ultrapure water. Viscosity standards (methyl cellulose viscosity 400 and porcine gastric mucin) were dissolved in electrolyte solutions at defined concentrations. Detailed compositions and preparation procedures are described in Section 1 of the Supplementary material.

2.2. Preparation of electrolyte solution

The electrolyte solution was prepared by diluting PBS with ultrapure water to obtain a final composition of 0.1 × PBS, 1 mM PF, and 2 M KCl in a total volume of 10 mL. A high ionic strength (2 M KCl) was used to suppress migration effects and maintain diffusion-controlled electrochemical behavior. This solution was defined as the blank solution. Viscosity standard solutions were prepared by adding methyl cellulose 400 or porcine gastric mucin to the blank solution at concentrations ranging from 1 to 256 mg L^{-1}.

For saliva analysis, real saliva was added to the blank solution instead of the viscosity standard substances to achieve a 500-fold dilution. All solutions were prepared immediately before the CV measurement.

2.3. Apparatus

CV was performed using an electrochemical measurement system (HZ-5000, Meiden Hokuto Corporation, Japan) with a standard three-electrode setup comprising a glassy carbon (GC) working electrode, platinum counter electrode, and Ag/AgCl reference electrode. Capillary electrophoresis was performed using chemically modified fused silica capillaries with capacitively coupled contactless conductivity detection (C^4D). Specific gravity was measured using a handheld refractometer and the TP concentration was determined using a Bradford assay. Detailed specifications and preparation procedures are provided in Section 2 of the Supplementary material.

2.4. Capillary electrophoresis

The anions and cations in saliva were analyzed separately using CE with the optimized buffer system described in a previous study [39]. Internal standards were included for each ion mode. Capillary preparation protocols and buffer compositions are described in Section 3 of the Supplementary material. The electropherograms of anions and cations optimized in this study are shown in Figs. S1 and S2, respectively. The analytical performances are summarized in Table S1.

Samples were introduced via hydrodynamic injection using a gravity-based method (7-cm height difference for 10 s). Internal standards were added to all samples, and ions were quantified based on the analyte-to-internal-standard peak area ratios to minimize variability associated with this method of sample introduction.

2.5. Saliva sample and cold pressor test

To evaluate the analytical performance of the ΔE_p-based viscosity correction, saliva samples were collected under CPT conditions, which are used as a physiological model of acute stress (Fig. 1). First, the repeated measurements were performed in a single healthy volunteer across eight independent sessions conducted between March and November 2024. In each session, saliva samples were collected 5 min before and 5 min after immersion of both hands in cold water (≤10 °C) or control water (37 °C) for 1 min. These repeated experiments were designed to examine intra-individual analytical variability and the effect of viscosity correction under controlled conditions.

In addition, the robustness of the correction strategy was evaluated in an independent cohort of 12 healthy participants, who were divided into a cold stimulation group ($n = 6$) and a control group ($n = 6$). Saliva samples were collected before and after the respective treatments using the same protocol. This cohort analysis was conducted to assess whether the ΔE_p-based correction improved differentiation of ion profiles under CPT conditions.

Approximately 2 mL of saliva was collected by the spitting method, centrifuged at 6714×g for 30 min at 25 °C, and the supernatant was

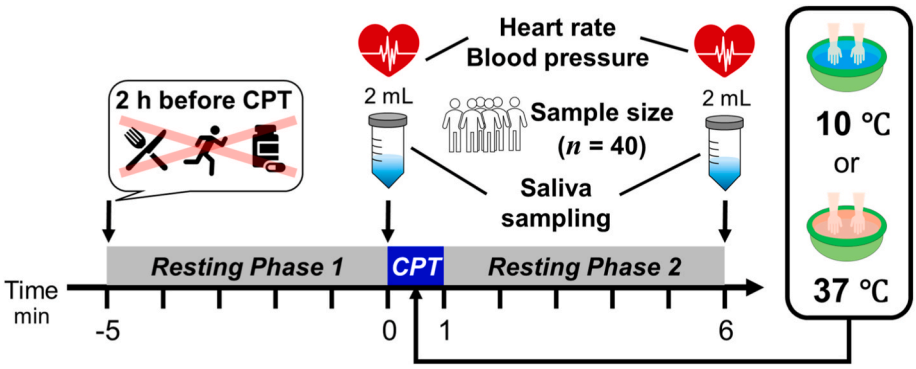

Fig. 1. Timeline of the cold pressor test procedure.

stored at −20 °C until analysis. All procedures were approved by the Kochi University Ethical Review Board (approval no. ERB-111751) and conducted in accordance with the Declaration of Helsinki.

Detailed collection protocols and ethical approval information are provided in Section 4 of the Supplementary material.

Participants were prohibited from oral intake for 2 h before CPT. Saliva samples were collected 5 min before and 5 min after the CPT/control procedure; the sample volumes were approximately 2 mL for each. A total of 40 samples were collected, including 16 samples comprising repeated measurements from one individual (8 independent trials × 2 samples) and 24 samples from an independent cohort of 12 healthy participants (6 cold stimulation and 6 control participants), each sampled before and after the procedure. The water temperature used for CPT was randomly selected for each participant.

2.6. Cyclic voltammetry

Before CV measurements, the GC working electrode was cleaned using 0.05 μm alumina on polishing pads (Buehler, Lake Bluff, Illinois). Then, the electrodes were rinsed with distilled water, sonicated in an ultrasonic bath for 1 min, and dried in air. Prior to each measurement, the sample solution was deoxygenated by bubbling with argon gas for 5 min. The peak potential difference (ΔE_p) was calculated using Eq. (1).

$$\Delta E_p = E_{pa} - E_{pc} \tag{1}$$

where E_{pa} and E_{pc} are the peak oxidation and peak reduction potentials, respectively. In this study, ΔE_p served as an indicator of the reversibility of the redox reaction of PF. The optimal ΔE_p is approximately 57 mV based on the Nernst equation [51]. The correction factor ($\Delta E_{p,r}$) was calculated using Eq. (2).

$$\Delta E_{p,r} = \Delta E_{p,0} / \Delta E_{p,i} \leq 1 \tag{2}$$

where $\Delta E_{p,0}$ and $\Delta E_{p,i}$ represent the ΔE_p obtained in the absence of saliva and in the presence of a 500-fold dilution of saliva, respectively. As the viscosity of saliva increases, $\Delta E_{p,i}$ rises, resulting in a CF < 1. The corrected ion concentration ($C_{ion,corr\_\Delta E_p}$) was calculated using Eq. (3).

$$C_{ion,corr\_\Delta E_p} = C_{ion,int.} \times CF \tag{3}$$

where $C_{ion,int.}$ represents the ion concentration obtained from CE measurements.

Each CV measurement was performed sequentially and the GC electrode was not polished between the blank and saliva solutions to maintain a constant electrode surface area.

2.7. Specific gravity measurement

Specific gravity was manually measured using a UG-α refractometer (ATAGO USA, Inc., Bellevue, WA, USA). Samples were equilibrated to room temperature prior to the measurement. The refractometer was calibrated with ultrapure water before use, cleaned with a lint-free tissue after each measurement, and recalibrated after every sample to ensure the accuracy of the measurements. Specific gravity normalization was performed using Eq. (4) as described in a previous study [45]:

$$C_{ion,corr\_S} = C_{ion,int.} \times (S_{target} - 1) / (S_{sample} - 1) \tag{4}$$

where S_{target} is defined as the target SG value of 1.0025 (mean value of saliva samples, $n = 16$). The SG of saliva is between 1.002 and 1.012, so this value is reasonable [56]. The S_{sample} value represents the measured SG of each individual sample. Although this correction method has been validated for urine samples, this represents its first application to saliva analysis.

2.8. Total protein concentration measurement (Bradford assay)

Total protein concentration was determined using the Bradford method [57] with bovine gamma globulin used as the standard. Absorbance was measured at 595 nm using a SpectraMax 190 microplate reader (Molecular Devices, LLC., San Jose, CA, USA). Total protein normalization was performed using Eq. (5) as described in a previous study [46].

$$C_{ion,corr\_T} = C_{ion,int.} \times T_{target} / T_{sample} \tag{5}$$

where T_{target} is defined as the target TP concentration of 0.614 mg mL^{-1} (mean values of saliva samples, $n = 16$). The TP in saliva is between 0.32 and 3.99 mg mL^{-1}, which is within the typical concentration [58,59]. T_{sample} represents the measured TP of each individual sample [60].

2.9. Viscosity measurement

The sample viscosity was measured using a rheometer and an Ostwald viscometer. Shear viscosity (η_s) of the samples (ca. 3 mL) was measured at 25 °C using a rheometer, equipped with a 25 mm diameter parallel plate. After equilibrating the sample at a shear rate of 100 s^{-1} for 1 min, η_s was obtained from the median of 90 consecutive measurements at a shear rate of 0.1 s^{-1}. Relative viscosity (η_r) of the samples (ca. 10 mL) was measured at 25 °C using an Ostwald viscometer. η_r was calculated from the ratio of the flow time of the sample (t) to that of the solvent (t_0).

2.10. Statistical analysis

All statistical analyses were performed using the Open-source Programming Language and Statistical Environment R (ver. R-4.1.1.tar.gz) [61]. Details of the statistical analyses and relative equations used in this study are detailed in Section 5 of the Supplementary material [62–64].

2.11. Safety Considerations

No unexpected, new, and/or significant hazards or risks were associated with the materials, chemicals, or procedures used in this study. All experiments—including electrochemical measurements, capillary electrophoresis, and handling of human saliva—were conducted in accordance with standard laboratory safety protocols and institutional guidelines for working with human-derived samples.

3. Results and discussion

3.1. Effect of mucin concentration on the peak area of CE

To examine the influence of mucin-induced viscosity on the peak areas of each ion, a mixed ion standard solution (0.01, 0.05, and 0.1 mmol L^{-1}) was prepared using four concentrations of mucin (0, 50, 100, and 200 mg L^{-1}) and analyzed by CE. A total of 14 ions were evaluated in this study: nine anions (Cl^-, NO_2^-, NO_3^-, SCN^-, HCO_3^-, HPO_4^{2-}, SO_4^{2-}, $HCOO^-$, and CH_3COO^-) and five cations (Na^+, K^+, NH_4^+, Mg^{2+}, and Ca^{2+}) that are common in human saliva [39].

As shown in Fig. S3, the peak areas of anions with relatively low electrophoretic mobility, such as HPO_4^{2-}, HCO_3^-, and CH_3COO^-, were affected by increased viscosity resulting from mucin concentrations in the sample solutions. In CE analysis, the injected sample migrates toward the detector as a zone, resulting in electrical dispersion [43]. According to the Stokes–Einstein equation [65], the diffusion coefficient (D) is inversely proportional to viscosity. Therefore, the reduced D values in highly viscous solutions resulted in diminished electrophoretic mobility for the analyte anions. Although the changes in peak areas were attributed to viscosity-induced diffusion effects, other factors may have also contributed. In particular, viscosity can affect the formation of the initial analyte zone before equilibration with the background electrolyte (BGE), leading to peak broadening. Interactions between mucin and certain ions (e.g., electrostatic binding or complex formation) could also influence the apparent peak areas independently of viscosity. Therefore, the observed behavior likely reflects a combination of viscosity-related diffusion effects [4,43] and ion–mucin interactions [40,66].

Similarly, all tested cations were affected by viscosity, with only Ca^{2+} exhibiting decreased peak areas at higher mucin concentrations (Fig. S3). This may be attributed to interactions with sialic acid residues present at the ends of the O-linked glycan chains of mucin molecules [40]. The behavior of Ca^{2+} suggests that specific interactions with mucin, such as binding to sialic acid residues, may also contribute to the observed changes. Polyvalent cations binding to sialic acid can alter mucin's tertiary structure and increase viscosity [66]. Because Ca^{2+} can bind at low concentrations (~1 mM), higher concentrations of polyvalent cations can further influence mucin viscosity. These complex interactions between mucin and inorganic ions may cause significant errors in the observed salivary ion concentrations.

It is generally accepted that, during CE separation, the viscosity of the analyte zone approaches that of the background electrolyte; thus, the steady-state signal is not directly governed by the initial sample viscosity. However, in practical CE analysis, the initial sample properties can still influence the analytical signal through injection-related effects and viscosity-dependent diffusion during the initial analyte zone formation.

First, in hydrodynamic injections, the injected sample volume depends on the solution viscosity, which can affect the amount of analyte introduced into the capillary. Therefore, viscosity-dependent variations in the injection volume cannot be completely excluded (refer to Fig. S4). However, an internal standard correction was applied to all analyses, aiming to reduce the impact of injection-volume variability on the calculated ion concentrations. Therefore, the observed changes should reflect not only differences in sample introduction, but also viscosity-related diffusions and, in some cases, ion–mucin interactions.

Second, the formation of the initial analyte zone is influenced by viscosity-dependent diffusion, which affects both peak shape and the dispersion of the analyte zone before reaching full equilibration with the BGE. In addition, possible interactions between mucin and analyte ions may influence the effective mobility and peak response.

Therefore, the observed changes in peak areas likely arose from the combined effects of injection-related variation, viscosity-dependent diffusion, and ion–mucin interactions, rather than from steady-state viscosity alone.

3.2. Relationship between mucin concentration and ΔE_p

Fig. 2 shows cyclic voltammograms of 1 mM $K_3[Fe(CN)_6]$ in the presence of designated mucin concentrations, and the obtained relationship between mucin concentration and ΔE_p. As the mucin concentration increased, the ΔE_p values rose and voltammogram peaks became laterally broader. The ΔE_p value strongly correlated with the logarithm of mucin concentration in the range of 1–256 mg L^{-1} ($\Delta E_p = 10.4 \ln [mucin] + 2.98$, $R^2 = 0.990$). This may partly reflect the increase in viscosity of the solution following the addition of mucin, which enhances flow resistance and prolongs the diffusion time in the bulk solution [67]. Under the present experimental conditions, the ferri/ferrocyanide redox system is expected to exhibit quasi-reversible behavior at the applied scan rate, allowing ΔE_p to reflect combined effects of diffusion and electron transfer kinetics [68].

While the diffusion coefficients (D) of PF decreased with increasing mucin concentrations (Table S2), the observed increase in ΔE_p and its saturation behavior in Fig. 2B indicate that factors beyond diffusion contribute to the electrochemical response.

In particular, possible interactions between mucin and the electrode surface or the redox probe may influence the effective electron transfer kinetics, which could contribute to the observed increase in ΔE_p [53]. Therefore, ΔE_p can be interpreted as reflecting the overall matrix effect, including both viscosity-related diffusion changes and additional interfacial or kinetic contributions. Based on this relationship, the ratio $\Delta E_{p,0}/\Delta E_{p,i}$ (Eq. (2)) is utilized as a correction factor (CF) to compensate for matrix-induced analytical bias (Eq. (3)).

In summary, ΔE_p serves as a practical indicator of the overall matrix effect within a physiologically relevant range, supporting its application as a robust correction factor in salivary ion analysis.

3.3. Correction of salivary ions using CF

Next, we measured a mixed ion standard solution (0.05 mmol L^{-1} each) using CE-C^4D and corrected the detected peak areas of each ion by applying the correction factor (CF) calculated from the relationship between ΔE_p and four mucin concentrations (0, 50, 100, and 200 mg L^{-1}). The ions that were strongly affected by mucin concentration in the absence of correction became nearly constant after applying the CF (Fig. S5). To further assess the validity of the proposed correction, selected cations and anions were analyzed using independent analytical methods (Fig. S6). For cations, atomic absorption spectrometry (AAS) yielded values closer to the ΔE_p-corrected CE results than to the uncorrected values. Because AAS atomizes analytes in a high-temperature environment, it is less affected by coexisting proteins or mucin-derived matrix components. These results support the interpretation that the ΔE_p-based correction effectively compensates for matrix-induced bias in CE cation analysis. Similarly, for most anions, ion chromatography (IC) results showed better agreement with the corrected values. Although both CE and IC are separation-based methods that may be influenced by organic matrices, the improved consistency after ΔE_p correction underscores the mitigation of diffusion-related errors. In contrast, the persistent underestimation only for Ca^{2+} is consistent with its specific chemical binding to mucin [40]. These results demonstrate the applied method's ability to distinguish between physical viscosity effects and specific chemical interactions. However, they also highlight a known limitation, i.e., the correction is ineffective for

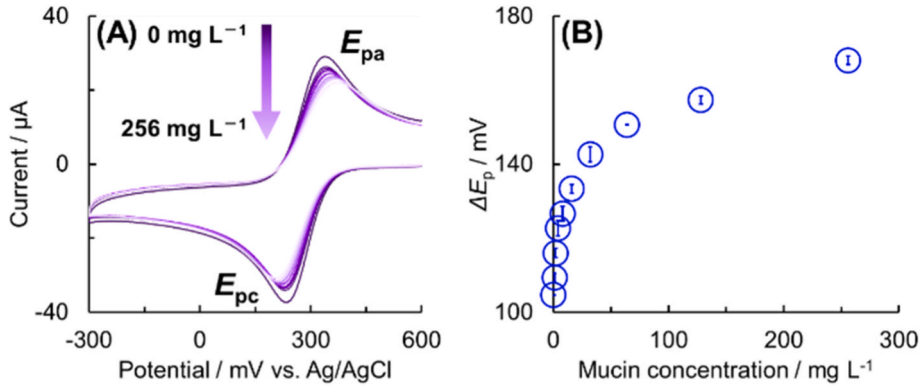

Fig. 2. (A) Cyclic voltammogram obtained at various mucin concentrations in 1 mM $K_3[Fe(CN)_6]$ solution (Blank solution) using a GC vs. Ag/AgCl electrode. (B) The relationship between mucin concentration and ΔE_p. All experiments were performed at a scan rate of 500 mV s^{-1}.

ions with a strong affinity for mucin. Crucially, viscosity effects persist even at dilutions exceeding 1000-fold, i.e., a level where analyte concentrations fall below the limit of detection (LOD) of the CE system rendering mathematical correction indispensable (Table S1). The applicable range of the proposed ΔE_p-based correction method corresponds to mucin concentrations in the range of 1–256 mg L^{-1}, within which there is a strong logarithmic relationship between ΔE_p and mucin concentration. Given that the mucin (MUC5B) concentration in actual saliva falls within the range of 308.1–445.2 mg L^{-1} [69], proper dilution (25-fold for anions and 100-fold for cations in this study) would nonetheless make this method effective for nearly all ions in practice.

3.4. Correlation between shear viscosity, relative viscosity, and ΔE_p

To compare ΔE_p with the results of viscosity measurements, two standard viscosity materials, methyl cellulose and mucin, were analyzed using a rheometer, an Ostwald viscometer and CV (Fig. 3). For methylcellulose, all parameters (η_s, η_r and ΔE_p) increased consistently with increasing concentration. In contrast, distinct discrepancies were observed for mucin depending on the measurement. While η_r (Fig. 3B) and ΔE_p (Fig. 3C) exhibited concentration-dependent increases, η_s (Fig. 3A) showed significant scattering, yielding no clear correlation. The consistent trends observed in the Ostwald and CV methods suggest that the viscosity of the mucin solution reliably increases with concentration. Therefore, the data scattering in the rheometer measurements is likely attributable to the structural characteristics of mucin.

Mucin is susceptible to mechanical stress [49]; specifically, the shear stress induced by the rotation of the rheometer plates may have destabilized the gel network structure formed by the mucin molecules [50]. In other words, it is difficult to dynamically measure the viscosity of a non-Newtonian fluid like mucin using a rheometer. Furthermore, it should be noted that Ostwald viscometers often exhibit measurement variability in low-viscosity regions approaching that of water, which may limit their precision for highly diluted samples. Cyclic voltammetry detects viscosity-induced changes in molecular diffusion as a static (non-mechanical) parameter. Therefore, ΔE_p responds sensitively to viscosity changes without physically disturbing the sample, making it a reliable indicator for evaluating the viscosity of mucin-containing samples, especially for non-Newtonian fluids such as saliva. Although ΔE_p was strongly correlated with mucin-induced viscosity, it may still be affected by experimental parameters such as scan rate, electrode surface condition, and probe stability. Thus, the calibration curve (Fig. 3C) should be interpreted as characteristic of electrochemical behavior in complex biological matrices rather than an absolute standard.

3.5. Variations in salivary ion concentrations using the cold pressor test

Storage stability tests confirmed that ΔE_p values for saliva and mucin remained stable at −20 °C for 7 days (Table S3), thus verifying that the results were not impacted by sample degradation. Variations in salivary

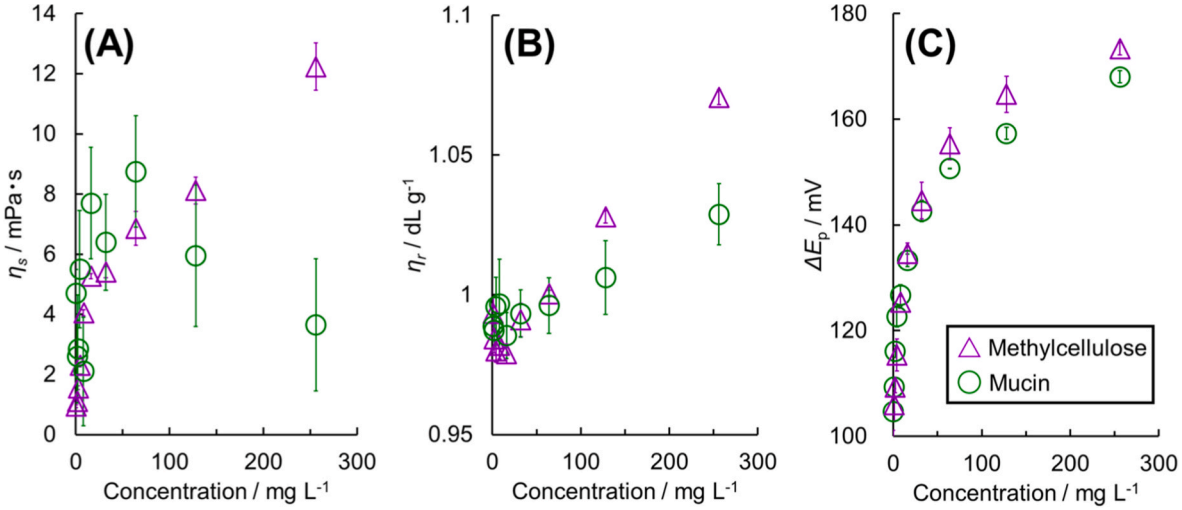

Fig. 3. Relationship between viscous standard substance concentration and shear viscosity (η_s), relative viscosity (η_r) and peak potential difference (ΔE_p). (A) Shear viscosity measured using a rheometer ($n = 90$), (B) Relative viscosity measured using an Ostwald viscometer ($n = 3$) and (C) ΔE_p measured by CV ($n = 5$). Mucin and methylcellulose are represented by ○ and △, respectively.

ion concentrations and physiological indicators (pH, TP, CF, SG, BP, and HR) before and after the CPT were visualized using slope graphs (Fig. S7 and Fig. 4). In repeated measurements, ΔE_p-based correction altered the apparent magnitude of ion concentration changes, indicating that viscosity-related diffusion effects contribute to analytical variability in CE measurements. Notably, CF values decreased after cold stimulation, whereas TP values increased (Fig. 4). Previous studies have shown that mucin secretion increases under low-temperature conditions [70], which would elevate sample viscosity and consequently reduce diffusion coefficients. Because ΔE_p reflects diffusion-controlled electrochemical behavior of the redox probe, the observed inverse relationship between TP and CF is consistent with increased viscosity influencing electrochemical peak separation.

To quantitatively compare normalization strategies, total anion and total cation concentrations were visualized as kernel density estimation (KDE) heatmaps (Fig. 5). A narrower distribution corresponds to reduced analytical dispersion. Compared with raw data (Fig. 5A), ΔE_p-based correction (Fig. 5B) produced a more compact distribution with approximately 1.5-fold higher clustering density, particularly for anions. This observation is consistent with diffusion-limited broadening predicted by the Stokes–Einstein relationship, where increased viscosity reduces diffusion coefficients and affects electrophoretic peak profiles.

The smaller improvement observed for cations may reflect partial binding of multivalent cations to sialic acid residues in mucin, which can modify effective mobility and conductivity response [66]. Such ion-specific interactions are not directly addressed by bulk normalization methods.

In contrast, SG-based normalization (Fig. 5C) improved cation clustering but broadened anion dispersion. Because SG relies on refractive index measurements influenced by hydration shells and ionic composition [71], it does not directly account for diffusion-related viscosity effects. TP-based normalization (Fig. 5D) increased variability for both ion classes, suggesting that total protein concentration does not linearly represent the diffusion behavior governing CE signal dispersion.

These results demonstrate that ΔE_p-based correction specifically mitigates viscosity-associated diffusion bias rather than merely scaling concentration values, thereby improving analytical robustness in mucin-rich matrices.

3.6. Principal component analysis

Principal component analysis (PCA) was performed to evaluate the effect of viscosity correction on multivariate ion profiles (Fig. 6). The single-individual dataset (Fig. 4) was integrated with an independent cohort of 12 healthy participants, resulting in a consolidated 40-sample dataset for the multivariate analysis. Within this complete dataset, the ΔE_p-corrected data (Fig. 6B) exhibited clearer separation between the cold stimulation and control conditions compared with the uncorrected data (Fig. 6A). Consequently, although the individual changes shown in Fig. 4 appeared modest when viewed in isolation, their combined variations were more clearly resolved within the multivariate PCA space. Loading plots revealed that PC1 was primarily driven by Ca^{2+}, NH_4^+ and Cl^- reflecting inter-individual variability. Specifically, PC2 functioned as an axis separating the cold and control groups, mainly driven by NO_3^-, SO_4^{2-}, SCN^- and HPO_4^{2-}. These ions exhibited strong negative factor loadings, indicating their collective decrease in response to the cold stimulation (Fig. S8). Importantly, the ΔE_p-correction facilitated the resolution of these CPT-related features within PC2, which were previously obscured by viscosity-induced noise in the uncorrected dataset.

This enhanced separation reflects a reduction in analytical variance rather than an artificial amplification of biological signals—a phenomenon consistent with shifts in PCA structure reported following normalization in metabolomic studies [72].

Rather than establishing definitive biomarkers, these identified ions represent stress-associated variations that become more detectable after correction of viscosity-induced bias. In particular, SO_4^{2-} and SCN^- showed increased loading contributions after correction. These ions are linked to hydrogen sulfide metabolism [73,74], which is associated with

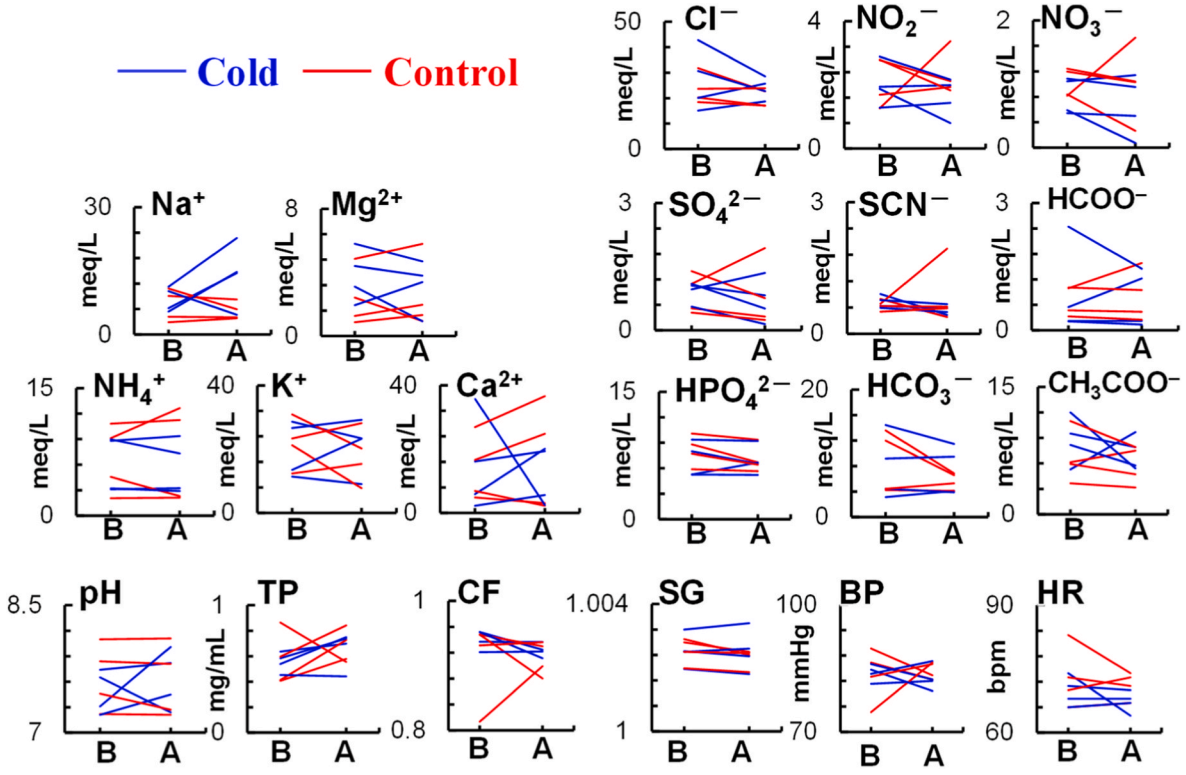

Fig. 4. Changes in the corrected concentrations of salivary ions (meq L^{-1}) before and after CPT ($n = 8$). Salivary pH values, total protein (TP) (mg mL^{-1}), correction factor (CF), specific gravity (SG), blood pressure (BP, mmHg), and heart rate (HR, bpm) before and after CPT ($n = 8$). X-axis: B = CPT and A = after CPT.

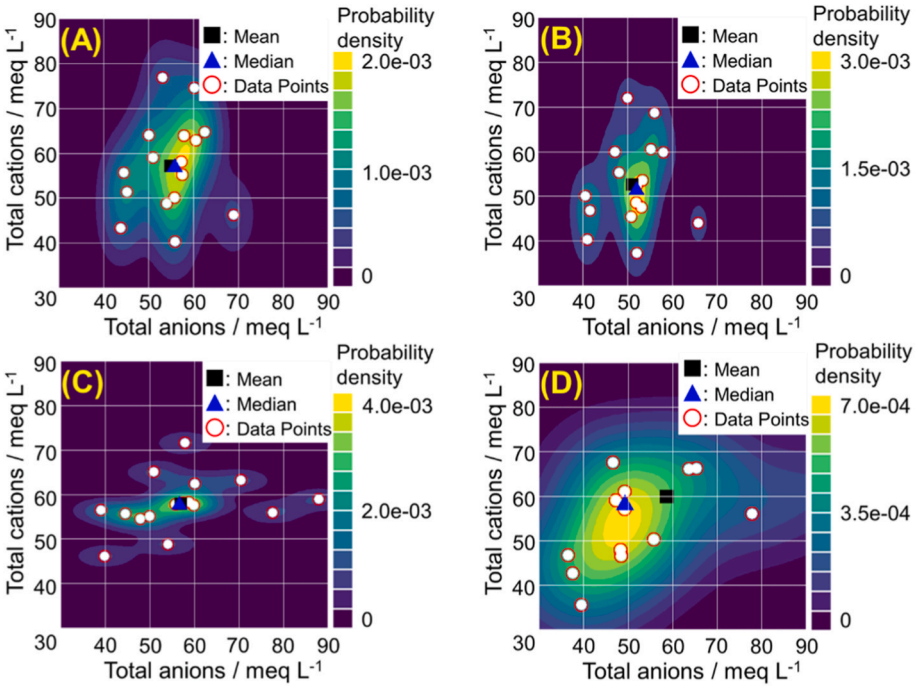

Fig. 5. Concentration distributions of total anions and cations represented by two-dimensional kernel density heat maps (A) before and (B) after correction by CF, (C) after correction by SG, and (D) after correction by TP. Open circles (○), filled squares (■), and filled triangles (▲) represent data points of salivary ion concentrations, mean values, and medians, respectively. Analyte data were obtained from 16 samples collected before and after CPT.

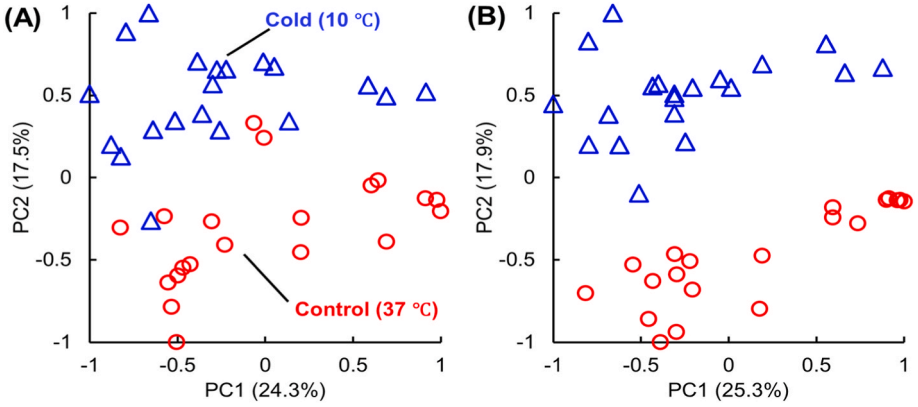

Fig. 6. The optimized score plot according to principal component analysis (A) before and (B) after CF application ($n = 40$). Open circles (○) and open triangles (△) represent the control groups and cold groups in the CPT, respectively. This plot consists of 14 ions.

vascular regulation.

Overall, the PCA results demonstrate that ΔE_p-based correction improves multivariate analytical stability and enhances the interpretability of ionomic data without artificially inflating group differences.

4. Conclusions

We developed an electrochemical viscosity-correction strategy based on the ΔE_p of a redox probe to mitigate diffusion-related bias in CE analysis of mucin-rich biofluids. By linking ΔE_p to sample-specific diffusion behavior, this method provides a rapid, non-destructive, and low-volume (10 μL) approach for correcting viscosity-associated analytical dispersion.

Application of the ΔE_p-based correction significantly improved the robustness and multivariate stability of salivary ion profiling compared with conventional normalization strategies such as specific gravity and total protein adjustment. In both repeated measurements and an independent cohort of healthy participants undergoing a CPT, the correction enhanced the detectability of stress-associated ion variations that were partially obscured in uncorrected data.

Rather than serving as a clinical diagnostic tool at this stage, the proposed strategy establishes an analytical framework for minimizing matrix-induced variability in complex biological samples. This approach is broadly applicable to other non-Newtonian biofluids and provides a foundation for improving reliability in ionomic analyses.

CRediT authorship contribution statement

Hironori Myochin: Conceptualization, Data curation, Formal analysis, Methodology, Writing – review & editing. **Romanas Chaleckis:** Conceptualization, Methodology, Writing – review & editing. **Tadaharu Ueda:** Conceptualization, Data curation, Formal analysis, Writing – review & editing. **Miguel Gonzálvez Noguera:** Data curation, Methodology. **Jie Zhang:** Data curation, Methodology, Writing – review &

editing. **Noriyasu Ohshima:** Data curation, Writing – review & editing. **Takashi Izumi:** Conceptualization, Writing – review & editing. **Tatsuya Hisajima:** Formal analysis, Writing – review & editing. **Mikaru Mori:** Data curation, Formal analysis. **Tomoya Kimura:** Data curation. **Masanobu Mori:** Conceptualization, Data curation, Formal analysis, Funding acquisition, Investigation, Methodology, Project administration, Resources, Supervision, Writing – original draft, Writing – review & editing.

Declaration of competing interest

The authors declare that they have no known competing financial interests or personal relationships that could have appeared to influence the work reported in this paper.

Acknowledgments

This work was supported by a Grant-in-Aid for Challenging Research (JP22K19733) from the Japan Society for the Promotion. We thank Artur Sawicki, PhD, from Edanz (https://jp.edanz.com/ac) for editing a draft of this manuscript.

Appendix A. Supplementary data

Supplementary data to this article can be found online at https://doi.org/10.1016/j.talanta.2026.129962.

Abbreviations

ΔE_p	peak potential separation
η	shear viscosity
η_r	relative viscosity
BP	blood pressure
C^4D	capacitively coupled contactless conductivity detection
CE	capillary electrophoresis
$C_{ion,corr\_\Delta E_p}$	corrected ion concentration
CPT	cold pressor test
CV	cyclic voltammetry
D	diffusion coefficient
E_{pa}	peak oxidation potential
E_{pc}	peak reduction potential
GC	glassy carbon
HR	heart rate
KDE	kernel density estimation
PBS	phosphate-buffered saline
PF	potassium ferricyanide
SG	specific gravity
TP	total protein

Data availability

Data will be made available on request.

References

[1] D. Bennet, Y. Khorsandian, J. Pelusi, A. Mirabella, P. Pirrotte, F. Zenhausern, Molecular and physical technologies for monitoring fluid and electrolyte imbalance: a focus on cancer population, Clin. Transl. Med. 11 (2021) e461, https://doi.org/10.1002/ctm2.461.

[2] K. Dhama, S.K. Latheef, M. Dadar, H.A. Samad, A. Munjal, R. Khandia, K. Karthik, R. Tiwari, M.I. Yatoo, P. Bhatt, S. Chakraborty, K.P. Singh, H.M.N. Iqbal, W. Chaicumpa, S.K. Joshi, Biomarkers in stress related diseases/disorders: Diagnostic, prognostic, and therapeutic values, Front. Mol. Biosci. 6 (2019) 91, https://doi.org/10.3389/fmolb.2019.00091.

[3] S. Qiu, Y. Cai, H. Yao, C. Lin, Y. Xie, S. Tang, A. Zhang, Small molecule metabolites: discovery of biomarkers and therapeutic targets, Signal Transduct. Target. Ther. 8 (2023) 132, https://doi.org/10.1038/s41392-023-01399-3.

[4] Z.K. Shihabi, Effect of sample composition on electrophoretic migration - application to hemoglobin analysis by capillary electrophoresis and agarose electrophoresis, J. Chromatogr. A 1027 (2004) 179–184, https://doi.org/10.1016/j.chroma.2003.08.054.

[5] J. Noiphung, M.P. Nguyen, C. Punyadeera, Y. Wan, W. Laiwattanapaisal, C. S. Henry, Development of paper-based analytical devices for minimizing the viscosity effect in human saliva, Theranostics 8 (2018) 3797–3807, https://doi.org/10.7150/thno.24941.

[6] D. Benni, K.M. Pallavi, T. Maddukuri, R. Singh, J.K. Gahlot, P. Basu, A. Kumari, Salivary diagnostics: bridging dentistry and medicine: a systematic review, Bioinformation 20 (2024) 1754–1759, https://doi.org/10.6026/9732063002001754.

[7] V. Shetty, C. Zigler, T.F. Robles, D. Elashoff, M. Yamaguchi, Developmental validation of a Point-of-Care, salivary α-Amylase biosensor, Psychoneuroendocrinology 36 (2011) 193–199, https://doi.org/10.1016/j.psyneuen.2010.07.008.

[8] A. Scarsi, D. Pedone, P.P. Pompa, A dual-color plasmonic immunosensor for salivary cortisol measurement, Nanoscale Adv. 5 (2022) 329–336, https://doi.org/10.1039/d2na00563h.

[9] A. Roda, S. Cavalera, F. Di Nardo, D. Calabria, S. Rosati, P. Simoni, B. Colitti, C. Baggiani, M. Roda, L. Anfossi, Dual lateral flow optical/chemiluminescence immunosensors for the rapid detection of salivary and serum IgA in patients with COVID-19 disease, Biosens. Bioelectron. 172 (2021) 112765, https://doi.org/10.1016/j.bios.2020.112765.

[10] D.H. Hellhammer, S. Wüst, B.M. Kudielka, Salivary cortisol as a biomarker in stress research, Psychoneuroendocrinology 34 (2009) 163–171, https://doi.org/10.1016/j.psyneuen.2008.10.026.

[11] T.D. Viena, J.B. Banks, I.M. Barbu, A.H. Schulman, J.L. Tartar, Differential effects of mild chronic stress on cortisol and S-IgA responses to an acute stressor, Biol. Psychol. 91 (2012) 307–311, https://doi.org/10.1016/j.biopsycho.2012.08.003.

[12] M.F. Larra, T.M. Schilling, P. Röhrig, H. Schächinger, Enhanced stress response by a bilateral feet compared with a unilateral hand cold pressor test, Stress 18 (2015) 589–596, https://doi.org/10.3109/10253890.2015.1053452.

[13] U.M. Nater, R. La Marca, L. Florin, A. Moses, W. Langhans, M.M. Koller, U. Ehlert, Stress-induced changes in human salivary alpha-amylase activity - associations with adrenergic activity, Psychoneuroendocrinology 31 (2006) 49–58, https://doi.org/10.1016/j.psyneuen.2005.05.010.

[14] S. Tsujita, K. Morimoto, Secretory IgA in saliva can be a useful stress marker, Environ. Health Prev. Med. 4 (1999) 1–8, https://doi.org/10.1007/BF02931243.

[15] A.M. Abdou, S. Higashiguchi, K. Horie, M. Kim, H. Hatta, H. Yokogoshi, Relaxation and immunity enhancement effects of γ-Aminobutyric acid (GABA) administration

in humans, Biofactors 26 (2006) 201–208, https://doi.org/10.1002/biof.5520260305.
[16] M. Uchida, T. Suga, M. Terada, T. Isaka, A pilot study: the relationship between salivary MCP-1 and IgA, and exercise performance in long-distance runners and sprinters, BMC Res. Notes 15 (2022) 118, https://doi.org/10.1186/s13104-022-05989-2.
[17] L. Manenschijn, J.W. Koper, S.W.J. Lamberts, E.F.C. Van Rossum, Evaluation of a method to measure long term cortisol levels, Steroids 76 (2011) 1032–1036, https://doi.org/10.1016/j.steroids.2011.04.005.
[18] A.M. Sesay, L. Micheli, P. Tervo, G. Palleschi, V. Virtanen, Development of a competitive immunoassay for the determination of cortisol in human saliva, Anal. Biochem. 434 (2013) 308–314, https://doi.org/10.1016/j.ab.2012.12.008.
[19] R. Kvietkauskaite, R. Vaicaitiene, M. Mauricas, The change in the amount of immunoglobulins as a response to stress experienced by soldiers on a peacekeeping mission, Int. Arch. Occup. Environ. Health 87 (2014) 615–622, https://doi.org/10.1007/s00420-013-0899-0.
[20] D. Li, R. Calderone, T.M. Nsouli, E. Reznikov, J.A. Bellanti, Salivary and serum IgA and IgG responses to SARS-CoV-2-Spike protein following SARS-CoV-2 infection and after immunization with COVID-19 vaccines, Allergy Asthma Proc. 45 (2022) 419–430, https://doi.org/10.2500/aap.2022.43.220045.
[21] I. Tsyrulneva, P. Alagappan, B. Liedberg, Colorimetric detection of salivary α-Amylase using maltose as a noncompetitive inhibitor for polysaccharide cleavage, ACS Sens. 4 (2019) 865–873, https://doi.org/10.1021/acssensors.8b01343.
[22] H.A. Silva-Neto, J.C. Jaime, D.S. Rocha, L.F. Sgobbi, W.K.T. Coltro, Fabrication of paper-based analytical devices using stencil-printed glass varnish barriers for colorimetric detection of salivary α-Amylase, Anal. Chim. Acta 1297 (2024) 342336, https://doi.org/10.1016/j.aca.2024.342336.
[23] J. Bakusic, S. De Nys, M. Creta, L. Godderis, R.C. Duca, Study of temporal variability of salivary cortisol and cortisone by LC-MS/MS using a new atmospheric pressure ionization source, Sci. Rep. 9 (2019) 19313, https://doi.org/10.1038/s41598-019-55571-3.
[24] Y. Peng, X. Chen, T. Sato, S.A. Rankin, R.F. Tsuji, Y. Ge, Purification and high-resolution top-down mass spectrometric characterization of human salivary α-Amylase, Anal. Chem. 84 (2012) 3339–3346, https://doi.org/10.1021/ac300083y.
[25] H.W. Chu, K.P. Chang, W.C. Yen, H.P. Liu, X.Y. Chan, C.R. Liu, C.M. Hung, C. C. Wu, Identification of salivary autoantibodies as biomarkers of oral cancer with immunoglobulin A enrichment combined with affinity mass spectrometry, Proteomics 23 (2023) 2200321, https://doi.org/10.1002/pmic.202200321.
[26] I. Restrepo-Angulo, C. Bañuelos, J. Camacho, Ion channel regulation by sex steroid hormones and vitamin D in cancer: a potential opportunity for cancer diagnosis and therapy, Front. Pharmacol. 11 (2020) 152, https://doi.org/10.3389/fphar.2020.00152.
[27] Y. Tanaka, N. Naruishi, H. Fukuya, J. Sakata, K. Saito, S.I. Wakida, Simultaneous determination of nitrite, nitrate, thiocyanate and uric acid in human saliva by capillary zone electrophoresis and its application to the study of daily variations, J. Chromatogr. A 1051 (2004) 193–197, https://doi.org/10.1016/j.chroma.2004.06.053.
[28] T. Miyado, Y. Tanaka, H. Nagai, S. Takeda, K. Saito, K. Fukushi, Y. Yoshida, S. I. Wakida, E. Niki, Simultaneous determination of nitrate and nitrite in biological fluids by capillary electrophoresis and preliminary study on their determination by microchip capillary electrophoresis, J. Chromatogr. A 1051 (2004) 185–191, https://doi.org/10.1016/j.chroma.2004.08.037.
[29] Z.F. Chen, B.W. Darvell, V.W.H. Leung, Human salivary anionic analysis using ion chromatography, Arch. Oral Biol. 49 (2004) 863–869, https://doi.org/10.1016/j.archoralbio.2004.05.002.
[30] I. Demkowska, Z. Polkowska, J. Namieśnik, Application of ion chromatography for the determination of inorganic ions, especially thiocyanates in human saliva samples as biomarkers of environmental tobacco smoke exposure, J. Chromatogr. B 875 (2008) 419–426, https://doi.org/10.1016/j.jchromb.2008.09.018.
[31] A.L. Suherman, B. Rasche, B. Godlewska, P. Nicholas, S. Herlihy, N. Caiger, P. J. Cowen, R.G. Compton, Electrochemical detection and quantification of lithium ions in authentic human saliva using $LiMn_2O_4$-Modified electrodes, ACS Sens. 4 (2019) 2497–2506, https://doi.org/10.1021/acssensors.9b01176.
[32] A. Dasca, P. Blondeau, J. Riu, F.J. Andrade, A paper-based organic electrochemical transistor array with a simplified configuration for simultaneous multi-ion detection, Talanta 282 (2025) 126957, https://doi.org/10.1016/j.talanta.2024.126957.
[33] E. Sundaram, K.L. Servarayan, V.S. Vasantha, Optical detection of thiocyanate in human saliva based on the colorimetric response of (2-(2-Hydroxyphenyl)-1H-Benzo[d]Imidazole-5-Yl)(Phenyl) methanone (HBPM)/Co^{2+} ions conjugate, Spectrochim. Acta 266 (2022) 120423, https://doi.org/10.1016/j.saa.2021.120423.
[34] L.R. Sousa, H.A. Silva-Neto, L.F. Castro, K.A. Oliveira, F. Figueredo, E. Cortón, W.K. T. Coltro, "Do It Yourself" protocol to fabricate dual-detection paper-based analytical device for salivary biomarker analysis, Anal. Bioanal. Chem. 415 (2023) 4391–4400, https://doi.org/10.1007/s00216-023-04581-2.
[35] M. Mori, W. Hu, K. Hasebe, S. Tanaka, K. Tanaka, Use of Phosphobetaine-Type zwitterionic surfactant for the determination of alkali and alkaline Earth metal ions and ammonium ion in human saliva by capillary electrophoresis, Anal. Bioanal. Chem. 374 (2002) 75–79, https://doi.org/10.1007/s00216-002-1434-4.
[36] M. Mori, M. Kaseda, T. Yamamoto, S. Yamada, H. Itabashi, Capillary ion electrophoresis-capacitively coupled contactless conductivity detection of inorganic cations in human saliva on a polyvinyl alcohol-coated capillary, Anal. Bioanal. Chem. 402 (2012) 2425–2430, https://doi.org/10.1007/s00216-011-5688-6.
[37] M. Mori, F. Ishikawara, T. Tomoda, S. Yamada, M. Okamoto, H. Itabashi, Y. Seki, R. Matsumoto, Y. Shoho, L. Martha, H. Sumino, M. Murakami, Use of capillary electrophoresis with dual-opposite end injection for simultaneous analysis of small ions in saliva samples from wrestlers undergoing a weight training program, J. Chromatogr. B 1012–1013 (2016) 178–185, https://doi.org/10.1016/j.jchromb.2016.01.037.
[38] M. Mori, K. Aoyagi, T. Tomoda, F. Ishikawara, S. Sakamoto, H. Myochin, M. Kuga, D. Kozaki, N. Ohshima, T. Izumi, H. Itabashi, Y. Shoho, A. Yoshida, K. Tsunekawa, T. Kimura, M. Murakami, Simultaneous capillary electrophoresis of anions and cations in a single injection using an anion exchanger-modified capillary for determination of salivary ions in combination with statistical analyses, J. Chromatogr. A 1635 (2021) 461647, https://doi.org/10.1016/j.chroma.2020.461647.
[39] H. Myochin, N. Ohshima, T. Izumi, T. Hisajima, R. Chaleckis, M. Mori, Capillary electrophoresis using triple layer modified capillary facilitating salivary ion analyses: application to search for potential stress markers induced by cold pressure test, J. Chromatogr. A 1720 (2024) 464769, https://doi.org/10.1016/j.chroma.2024.464769.
[40] S. Takehara, M. Yanagishita, K.A. Podyma-Inoue, Y. Kawaguchi, Degradation of MUC7 and MUC5B in human saliva, PLoS One 8 (2013) e69059, https://doi.org/10.1371/journal.pone.0069059.
[41] H. Inoue, K. Ono, W. Masuda, T. Inagaki, M. Yokota, K. Inenaga, Rheological properties of human saliva and salivary mucins, J. Oral Biosci. 50 (2008) 134–141, https://doi.org/10.1016/S1349-0079(08)80027-8.
[42] S. Hjertén, Free zone electrophoresis, chromatogr, Rev. 9 (1967) 122–219, https://doi.org/10.1016/0009-5907(67)80003-6.
[43] A. Allmendinger, L.H. Dieu, S. Fischer, R. Mueller, H.C. Mahler, J. Huwyler, High-throughput viscosity measurement using capillary electrophoresis instrumentation and its application to protein formulation, J. Pharm. Biomed. Anal. 99 (2014) 51–58, https://doi.org/10.1016/j.jpba.2014.07.005.
[44] M. Swaminathan, A. Tarifa, A.P. DeCaprio, Development and validation of a method for analysis of 25 cannabinoids in oral fluid and exhaled breath condensate, Anal. Bioanal. Chem. 416 (2024) 4325–4340, https://doi.org/10.1007/s00216-024-05369-8.
[45] I. Meister, P. Zhang, A. Sinha, C.M. Sköld, Å.M. Wheelock, T. Izumi, R. Chaleckis, C.E. Wheelock, High-precision automated workflow for urinary untargeted metabolomic epidemiology, Anal. Chem. 93 (2021) 5248–5258, https://doi.org/10.1021/acs.analchem.1c00203.
[46] A. Maloy, S. Alexander, A. Andreas, T. Nyunoya, D. Chandra, Stain-Free total-protein normalization enhances the reproducibility of Western blot data, Anal. Biochem. 654 (2022) 114840. https://dx.doi.org/10.1016/j.ab.2022.114840.
[47] A.J. Chetwynd, A. Abdul-Sada, S.G. Holt, E.M. Hill, Use of a pre-analysis osmolality normalisation method to correct for variable urine concentrations and for improved metabolomic analyses, J. Chromatogr. A 1431 (2016) 103–110, https://doi.org/10.1016/j.chroma.2015.12.056.
[48] Y. Wu, L. Li, Sample normalization methods in quantitative metabolomics, J. Chromatogr. A 1430 (2016) 80–95, https://doi.org/10.1016/j.chroma.2015.12.007.
[49] M. Ahmad, C. Ritzoulis, J. Chen, Shear and extensional rheological characterisation of mucin solutions, Colloids Surf. B Biointerfaces 171 (2018) 614–621, https://doi.org/10.1016/j.colsurfb.2018.07.075.
[50] C.E. Wagner, G.H. McKinley, Age-dependent capillary thinning dynamics of physically-associated salivary mucin networks, J. Rheol. 61 (2017) 1309–1326, https://doi.org/10.1122/1.4997598.
[51] N. Elgrishi, K.J. Rountree, B.D. McCarthy, E.S. Rountree, T.T. Eisenhart, J. L. Dempsey, A practical beginner's guide to cyclic voltammetry, J. Chem. Educ. 95 (2018) 197–206, https://doi.org/10.1021/acs.jchemed.7b00361.
[52] P. Krishnaveni, V. Ganesh, Electron transfer studies of a conventional redox probe in human sweat and saliva bio-mimicking conditions, Sci. Rep. 11 (2021), https://doi.org/10.1038/s41598-021-86866-z.
[53] T.J. Davies, et al., A computational and experimental study of the cyclic voltammetry response of partially blocked electrodes. Part II: randomly distributed and overlapping blocking systems, J. Phys. Chem. B 107 (2003) 6431–6444, https://doi.org/10.1021/jp022616b.
[54] E.A. Hines, G.E. Brown, The cold pressor test for measuring the reactibility of the blood pressure: data concerning 571 normal and hypertensive subjects, Am. Heart J. 11 (1936) 1–9, https://doi.org/10.1016/S0002-8703(36)90370-8.
[55] L. Schwabe, L. Haddad, H. Schachinger, HPA axis activation by a socially evaluated cold-pressor test, Psychoneuroendocrinology 33 (2008) 890–895, https://doi.org/10.1016/j.psyneuen.2008.03.001.
[56] E. Kubala, P. Strzelecka, M. Grzegocka, D. Lietz-Kijak, H. Gronwald, P. Skomro, E. Kijak, A review of selected studies that determine the physical and chemical properties of saliva in the field of dental treatment, Biomed Res. Int. 2018 (2018) 13, https://doi.org/10.1155/2018/6572381.
[57] M.M. Bradford, A rapid and sensitive method for the quantitation of microgram quantities of protein utilizing the principle of protein-dye binding, Anal. Biochem. 72 (1976) 248–254, https://doi.org/10.1016/0003-2697(76)90527-3.
[58] F. Michishige, K. Kanno, S. Yoshinaga, D. Hinode, Y. Takehisa, S. Yasuoka, Effect of saliva collection method on the concentration of protein components in saliva, J. Med. Investig. 53 (2006) 140–146, https://doi.org/10.2152/jmi.53.140.
[59] H. Jasim, P. Olausson, B. Hedenberg-Magnusson, M. Ernberg, B. Ghafouri, The proteomic profile of whole and glandular saliva in healthy pain-free subjects, Sci. Rep. 6 (2016) 39073, https://doi.org/10.1038/srep39073.

[60] K. Al-Manei, N. Almotairy, N. Bostanci, A. Kumar, A. Grigoriadis, Effect of chewing on the expression of salivary protein composition: a systematic review, Proteom. - Clin. Appl. 14 (2020) 1900039, https://doi.org/10.1002/prca.201900039.
[61] The open-source programming language and statistical environment R (ver. R-4.1.1.tar.gz). https://cran.r-project.org/src/base/R-4/. (Accessed 30 June 2025).
[62] S. Węglarczyk, Kernel density estimation and its application, ITM Web Conf. 23 (2018) 00037, https://doi.org/10.1051/itmconf/20182300037.
[63] S. Ren, A.A. Hinzman, E.L. Kang, R.D. Szczesniak, L.J. Lu, Computational and statistical analysis of metabolomics data, Metabolomics 11 (2015) 1492–1513, https://doi.org/10.1007/s11306-015-0823-6.
[64] H. Abdi, L.J. Williams, Principal component analysis, Comput. Stat. 2 (2010) 433–459, https://doi.org/10.1002/wics.101.
[65] A. Einstein, Über Die von Der Molekularkinetischen Theorie Der Wärme Geforderte Bewegung von in Ruhenden Flüssigkeiten Suspendierten Teilchen, Ann. Phys. 322 (1905) 549–560, https://doi.org/10.1002/andp.19053220806.
[66] A. Curnutt, K. Smith, E. Darrow, K.B. Walters, Chemical and microstructural characterization of pH and [Ca^{2+}] dependent sol-gel transitions in Mucin biopolymer, Sci. Rep. 10 (2020) 8760, https://doi.org/10.1038/s41598-020-65392-4.
[67] M. Kergoat, M. Gibilaro, L. Massot, P. Chamelot, Generalized method for determining fluoroacidity by electrochemical diffusion coefficient measurement (application to HfF4), Electrochim. Acta 176 (2015) 265–269, https://doi.org/10.1016/j.electacta.2015.06.124.
[68] R. Agarwal, The Nicholson method of determination of the standard rate constant of a quasireversible redox couple employing cyclic voltammetry: everything one needs to know, ACS Electrochem 1 (2025) 1885–1894, https://doi.org/10.1021/acselectrochem.5c00214.
[69] M. Faruque, M. Wanschers, A.J. Ligtenberg, M.L. Laine, F.J. Bikker, A review on the role of salivary MUC5B in oral health, J. Oral Biosci. 64 (2022) 392–399, https://doi.org/10.1016/j.job.2022.09.005.
[70] A.J.M. Ligtenberg, M. Meuffels, E.C.I. Veerman, Effects of environmental temperature on saliva flow rate and secretion of protein, amylase and mucin 5B, Arch. Oral Biol. 109 (2020) 104593, https://doi.org/10.1016/j.archoralbio.2019.104593.
[71] M.N. Kammer, A.K. Kussrow, D.J. Bornhop, Theoretical basis for refractive index changes resulting from solution phase molecular interaction, J. Phys. Chem. B 129 (2025) 3297–3305, https://doi.org/10.1021/acs.jpcb.4c07563.
[72] W. Han, L. Li, Evaluating and minimizing batch effects in metabolomics, Mass Spectrom. Rev. 41 (2022) 421–442, https://doi.org/10.1002/mas.21672.
[73] M. Libiad, A. Sriraman, R. Banerjee, Polymorphic variants of human Rhodanese exhibit differences in thermal stability and sulfur transfer kinetics, J. Biol. Chem. 290 (2015) 23579–23588, https://doi.org/10.1074/jbc.M115.675694.
[74] G. Cirino, C. Szabo, A. Papapetropoulos, Physiological roles of hydrogen sulfide in Mammalian cells, tissues, and organs, Physiol. Rev. 103 (2023) 31–276, https://doi.org/10.1152/physrev.00028.2021.